Received: 03 June 2021 | Revised: 09 July 2021 | Accepted: 02 August 2021
DOI: 10.22034/ecc.2021.293399.1196
Eurasian Chemical Communications
SAMI

FULL PAPER

Hydrothermal synthesis and characterization of zinc sulfide nanoparticles

Alaa Abd AL-Zahra* |Abdul Karim M. A. Al-Sammarraie

Department of Chemistry, College of Science, University of Baghdad, Baghdad, Iraq

***Corresponding Author:**
Alaa Abd AL-Zahra
Email: thechimalaa@gmail.com
Tel.: +009647710990213

Zinc sulfide NPs are well-known as excellent photo catalyst because of their unique optical properties such as band gap energy, retention time, the high light absorption, electron-hole recombination time, and high negative reduction-oxidation potential of excited electrons. Nanoparticles of (ZnS) were synthesized successfully from the reaction of a mixture of zinc chloride ($ZnCl_2$) as precursor, ammonium nitrate (NH_4NO_3) and different concentrations of potassium hydroxide oxide (KOH) with drop wise added thiourea ($CS(NH_2)_2$) in a hydrothermal Teflon-lined stainless-steel bomb at temperature of 120 ^oC. Particle size and surface morphology of the prepared ZnS nanoparticles were calculated using Scanning Electron Microscopy (SEM) and Atomic Force Microscopy (AFM), they show a ZnS spherical particle with diameters around 60 nm. X-Ray diffraction (XRD) revealed a ZnS cubical crystal structure. Fourier transforms infrared (FTIR) spectroscopic analysis show the zinc to sulfur band at 627 cm^{-1}. The absorption spectra of ZnS NPs in the ultraviolet and visible ranges show a blue at λ_{max} of 302 nm.

KEYWORDS

Zinc sulfide nanoparticle; hydrothermal method; atomic force microscopy (AFM); UV-visible spectroscopy; X-ray diffraction (XRD); scanning electron microscopy (SEM).

Introduction

Zinc sulfide is a useful II-IV semiconductor compound having a tiny band gap at 300 K, the cubic zinc blende phase has 3.72 eV, while the hexagonal wurtzite phase has 3.77 eV and a high exaction binding energy of 40 meV [1]. It is used in optical sensors [2], catalysts [3], photoconductors [4], phosphors [5], and solid-state solar window layers [6], among other things. In order to attain desired physical qualities, it has been widely explored to monitor the size, shape, and crystallinity of ZnS Nano crystals. ZnS has been synthesized using a variety of methods electrochemical deposition [7], micro emulsion [8], solvothermal [9], sol-gel [10,11], co precipitation [12,13], vapor deposition [14], laser ablation, [15], hydrothermal [16], pyrolysis [17] and combustion synthesis [18]. This work describes the synthesis and characteristics of zinc sulphide nanoparticles produced by a hydrothermal technique under varied reaction circumstances. This is a straight forward approach for making Nano crystals under high heats and pressures, from aqueous solutions. Two advantages of this technique over others are the capacity to manufacture crystalline phases that are not stable at melting temperatures and materials with a high vapor pressure at their melting points. The main goal of the current research is to determine the impact of synthesis conditions on the crystal structure, shape, and size of ZnS products.

Experimental

The hydrothermal process was carried out in an autoclave, which was steel cylinder with a thick wall that was sealed hermetically to withstand high pressures and temperatures for long intervals of time. A Teflon vessel, used to resist corrosion, was inserted into the autoclave's internal cavity. The vessel was outfitted with a 30 mm inner diameter and a 120 mL volume. Many of the compounds were of the analytical variety and they were without any additional purification. The experiments were carried out using various composition concentrations at 120 ^{o}C [19]. Experiment details were as follows:

80 mL of (0.02 M) $ZnCl_2$, 80 mL of (1.5 M) NH_4NO_3 and 200 mL of (0.9 M, 1 M, 1.2 M and 1.4 M) KOH were dissolved in de-ionized water separately and agitated for 10 minutes at room temperature. Then, they were mixed through dripping 80 mL of (0.2 M) CS $(NH_2)_2$ solution drops into mixture solution while stirring.

The mixture was put into a stainless-steel autoclave with Teflon coating, after that it was filled to 40% capacity using a mixed solution. It was placed at a temperature of 120 °C for 12 hours, and then cooled to room temperature naturally. After centrifuging the product-containing solution, it was washed with distilled water twice. To extract impurities in the sample, the washing process was carried out ten times. The resulting white product was dried out for 6 hours in a 60 °C oven.

X-ray diffraction was used to investigate the structure of the ZnS samples using a Siemens model D500, SEM ZEISS model: sigma VPEDS and mapping: oxford instruments, UK.

Shimadzu UV 1800 twin beam, Japan, area (200-1100) nm, was used to get the absorption spectra, and to analyze the composition and quality of the compound in the rang (4000-400 cm^{-1}) the Fourier transform infrared spectroscopy (FTIR) Shimadzu FT-IR8400S, Japan was applied.

Result and discussion

A: XRD analysis

XRD patterns in Figure 1 clearly show cubical crystalline structure of all prepared Nano sized ZnS samples as the indexed Peaks at 2Θ=(28.67^{o}, 33.1^{o}, 47.6^{o}, and 56.4^{o}, respectively, correspond to (111), (200), (220), and (311) planes, and match the stated value (JCPDS card, No. 5-0566) [20].

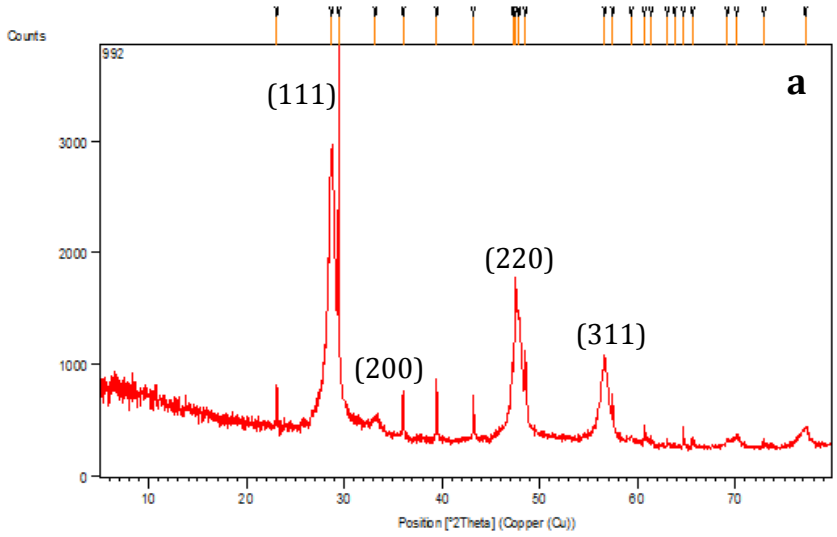

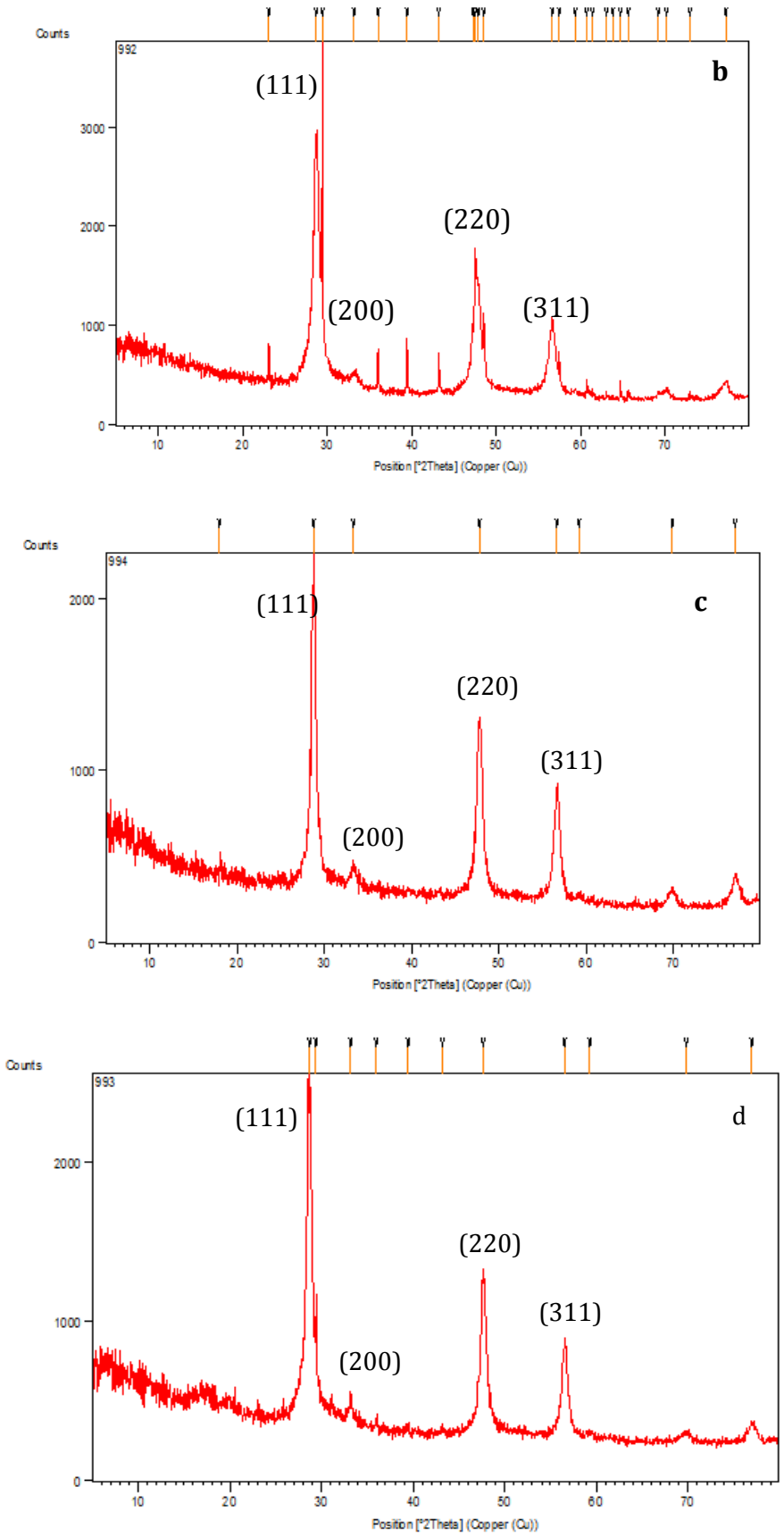

FIGURE 1 XRD patterns of ZnS nanostructures in different concentration of KOH (a: 0.9M, b: 1M, c: 1.2 M and d: 1.4 M)

The calculated lattice parameters are listed in Table 1. The peaks' broad appearance implies that the crystal size is in the nanometer rang. The Wulf - Bragg relation is used to compute the distances d_{hkl} between successive lattice planes:

$2d_{hkl} \sin\theta = n\lambda$ … (1)

The Debye – Scherrer equation was used to compute the average crystalline size of the powder. [21,22]:

$D=0.9\lambda/\beta\cos\theta$… (2)

where the wavelength of X-ray λ= (0.154 nm), the angle of incidence is (θ). The order of the corresponding reflection is denoted by the integer n, D is the mean crystallite size, and β is the whole width of the XRD peak appearing at the diffraction angle at half maximum.

For samples (a), (b), (c), and (d), the average crystallite size of ZnS nanoparticles was found to be (40 nm, 61 nm, 39 nm, and 45 nm, respectively.

TABLE 1 Nano crystal sizes and Lattice constants calculated from XRD (λ=0.154 nm) patterns for samples a, b, c and sample d

sample	plane	2θ(degree)	(Interplanar distance) d= λ/2sin θ	FWHM (β) (degree)	D (nm)
	111	28.69	0.318	0.415	40
a	220	47.25	0.1921	0.28	
	311	56.25	0.1623	0.5	
	111	28.67	0.311	0.15	61
b	220	47.62	0.190	0.32	
	311	56.53	0.1626	0.375	
	111	28.76	0.3101	0.35	39
c	220	47.77	0.1901	0.42	
	311	56.62	0.1623	0.39	
	111	28.691	0.31085	0.25	45
d	220	47.718	0.1904	0.38	
	311	56.60	0.1624	0.40	

B: SEM images

The SEM images for the samples a, b, c, and d reflect spherical ZnS particles with diameters around 40, 50, 45, and 55 nm, respectively.

These images revealed small effect of KOH concentrations on the shape or diameters of the ZnS grains [23].

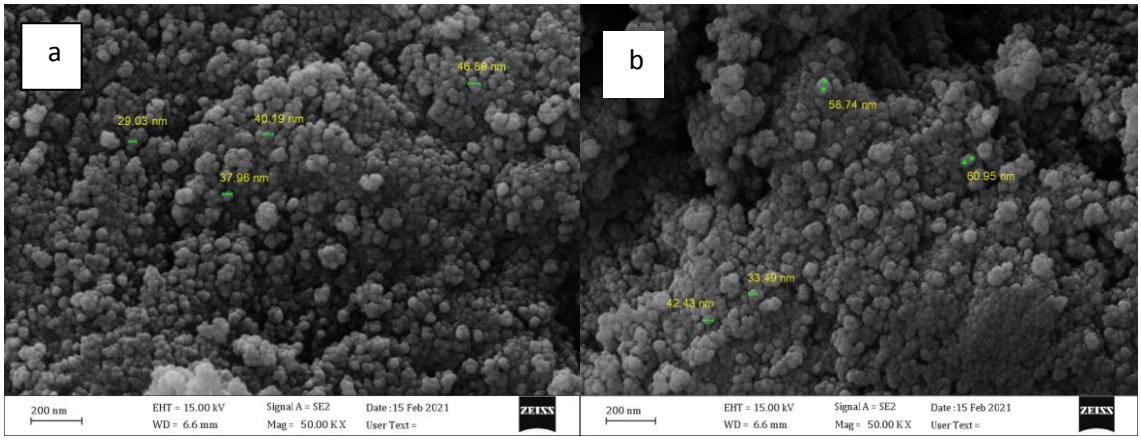

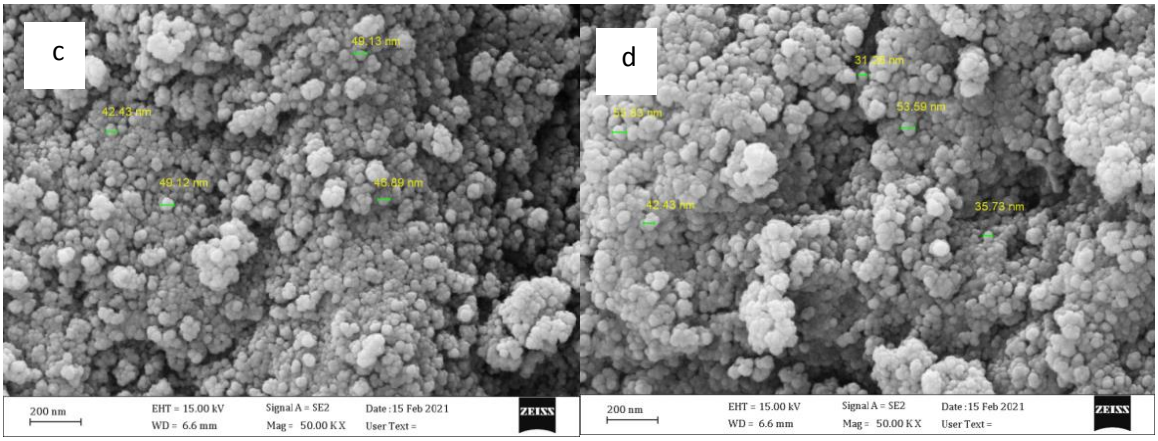

FIGURE 2 SEM images of ZnS nanostructures prepared at different concentration of KOH

C. AFM analysis

Figure 3 shows 2D and 3D AFM images, also reflected nearly spherical particles with a diameter somehow less than the observed by SEM images for all prepared ZnS and they are around 35 nm. The only differences noticed are with the particle size distribution profile and the values of the particles roughness, which increased with increasing the concentration of the KOH.

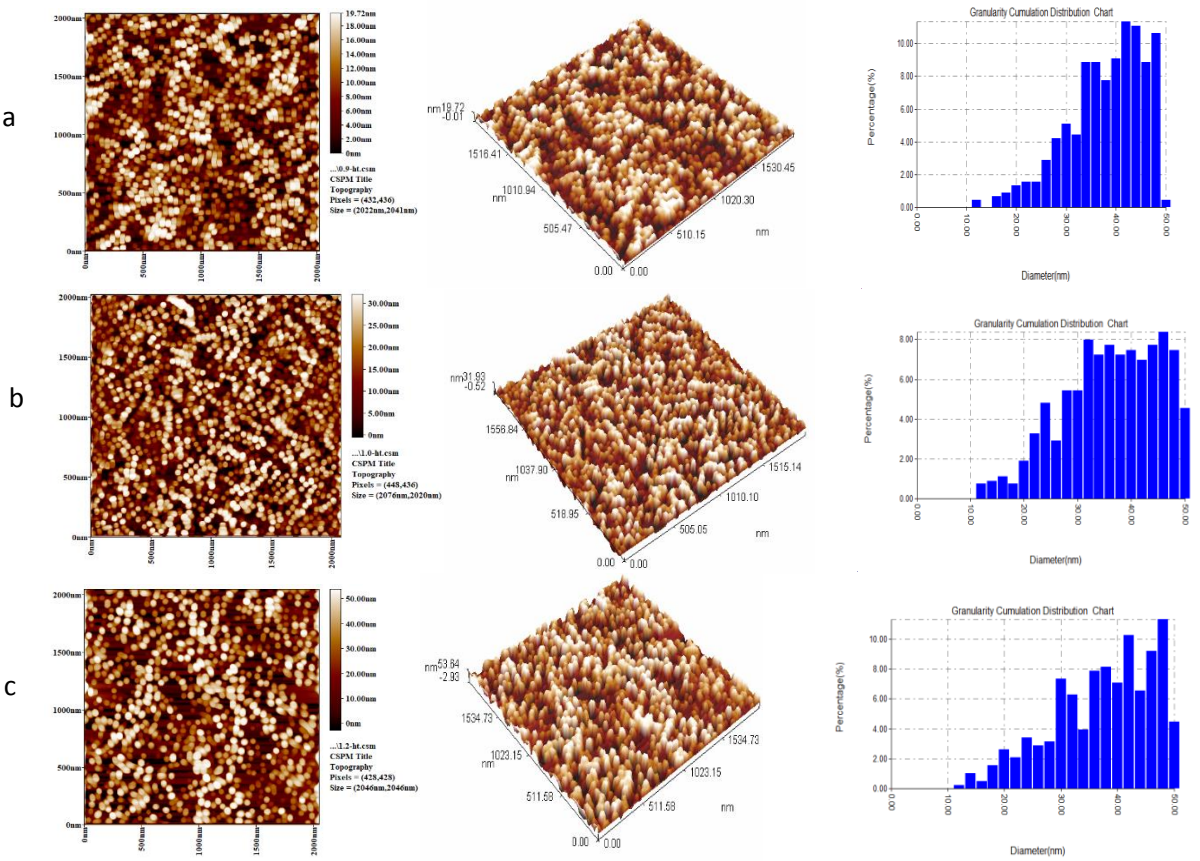

d

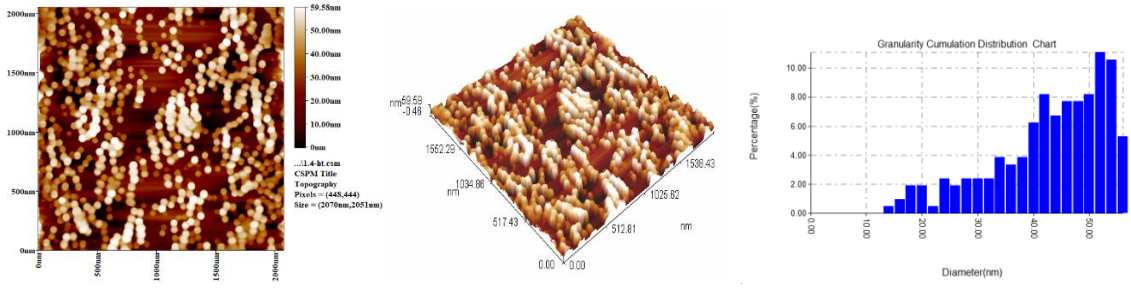

FIGURE 3 2D, 3D images and the particle size distribution profile of ZnS nanostructures prepared at different concentration of KOH

D. UV-VIS spectra

The UV-VIS spectra of ZnS samples are shown in Figure 3. It shows a strong absorption peak by ZnS around 400 nm corresponding to the optical band gap [24,25].

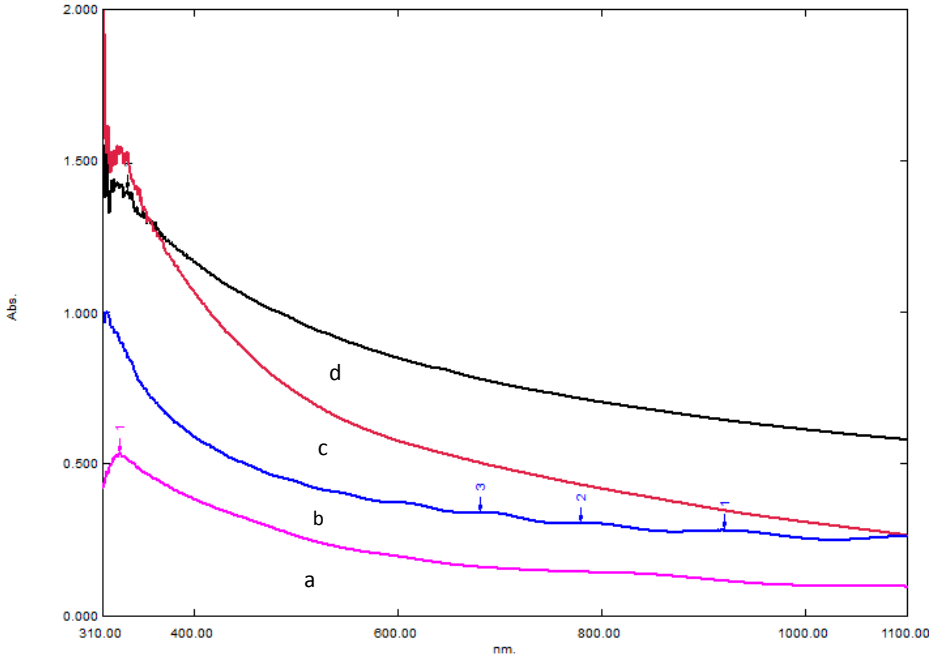

FIGURE 4 Absorption spectra for ZnS nanostructures prepared at different KOH concentration

E. FTIR spectra

The FTIR spectra of the four ZnS samples seems to be very identical (Figure 5). The significant bands are at 1000 and 657 cm^{-1}, respectively, and are the result of characteristic Zn-S stretching and vibration [26]. Bands around 3160-3226, 3420-3550 cm^{-1} belong to the hydrogen frequency of stretching (OH stretching) of the hydroxyl group [27], bands around 1630 cm^{-1} are due to the C–O vibrational modes arise from absorbed CO_2 on the surface of the nano crystals [28].

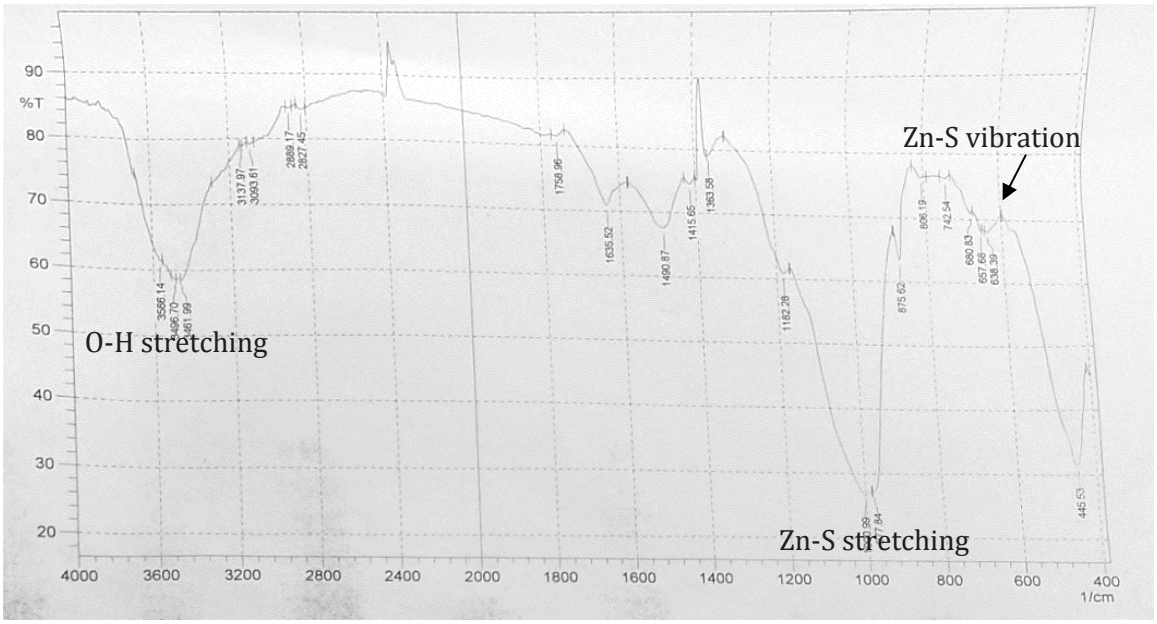

FIGURE 5 FTIR Spectrum of ZnS powder prepared by hydrothermal techniques

Conclusion

Nano crystalline ZnS have been successfully synthesized by a hydrothermal method at 120 °C and 12 h under different concentration of KOH. X-ray diffraction studies revealed that the synthesized particles have cubic zinc blende structure; the average crystallite size of ZnS nanoparticles was found to be 40 nm, 61 nm, 39 nm, and 45 nm for different KOH concentration. The absorption spectra of ZnS NPs in the ultraviolet and visible ranges show a blue at λ max of 302 nm.

Acknowledgements

I would like to thank all member staff of department of Chemistry, University of Baghdad.

Orcid:
Abdul Karim M. A. Al-Sammarraie:
https://orcid.org/0000-0002-3983-1608

References

[1] P. D'Amico, A. Calzolari, A. Ruini, A. Catellani, *Sci. Rep.*, **2017**, *7*, 1–9. [crossref], [Google Scholar], [Publisher]
[2] G.S. Rodríguez, R.C.C. Torres, R.S. Zeferino, M.E.A. Ramos, *Opt. Mater.*, **2019**, *89*, 396–401. [crossref], [Google Scholar], [Publisher]
[3] A. Wei, J. Liu, M. Zhuang, Y. Zhao, *Mater. Sci. Semicond. Process.*, **2013**, *16*, 1478–1484. [crossref], [Google Scholar], [Publisher]
[4] R.A. Faris, S.K. Al-Hayali, A.H. Al-Janabi, *Opt. Commun.*, **2021**, *485*, 126746. [crossref], [Google Scholar], [Publisher]
[5] A.M.T. Allayla, R.A. Faris, Z.F. Mahdi, *Vib. Spectrosc.*, **2021**, *114*, 103252. [crossref], [Google Scholar], [Publisher]
[6] J.K. Lee, G.J. Sun, W.S. Lee, S.K. Hyun, K.K. Kim, S.B. Choi, C. Lee, *Sci. Rep.*, **2017**, *7*, 1–8. [crossref], [Google Scholar], [Publisher]
[7] B. Altıokka, *J. Electron. Mater.*, **2019**, *48*, 2398–2403. [crossref], [Google Scholar], [Publisher]
[8] T. Charinpanitkul, A. Chanagul, J. Dutta, U. Rungsardthong, W. Tanthapanichakoon, *Sci. Technol. Adv. Mater.*, **2005**, *6*, 266–271. [crossref], [Google Scholar], [Publisher]
[9] L. Yu, H. Ruan, Y. Zheng, D. Li, *Nanotechnology*, **2013**, *24*, 375601–375610. [crossref], [Google Scholar], [Publisher]
[10] A. Tounsi, D. Talantikite-Touati, R. Khalfi, H. Merzouk, H. Haddad, *Proc. Third Int. Symp.*

Mater. Sustainable Dev., **2018**, 44–51. [crossref], [Google Scholar], [Publisher]
[11] A. Goktas, A. Tumbu, F. Aslan, *J. Sol-Gel Sci. Technol.*, **2019**, *90*, 487–497. [crossref], [Google Scholar], [Publisher]
[12] G. Mahesh, M. Venkatachalam, M. Saroja, M. Balachander, *Int. J. Res. App. Sci. Eng. Tech.*, **2018**, *5*, 1852–1855. [Pdf], [Google Scholar], [Publisher]
[13] N. Shanmugam, S. Cholan, N. Kannadasan, K. Sathishkumar, G. Viruthagiri, *Solid State Sci.*, **2014**, *28*, 55-60. [crossref], [Google Scholar], [Publisher]
[14] A. Varma, A.S. Mukasyan, A.S. Rogachev, K.V. Manukyan, *Chem. Rev.*, **2016**, *116*, 14493-14586. [crossref], [Google Scholar], [Publisher]
[15] M. Hrubaru, D.C. Onwudiwe, E. Hosten, *J. Sulfur Chem.*, **2016**, *37*, 37-47. [crossref], [Google Scholar], [Publisher]
[16] V. Sabaghia, F. Davara, Z. Fereshteh, *Ceramics Int.*, **2018**, *44*, 7545–7556. [crossref], [Google Scholar], [Publisher]
[17] M. Jadraque, A.B. Evtushenko, D. Ávila-Brande, M. López-Arias, V. Loriot, Y.G. Shukhov, L.S. Kibis, A.V. Bulgakov, M. Martín, *J. Phy. Chem. C*, **2013**, *117*, 5416–5423. [crossref], [Google Scholar], [Publisher]
[18] A.M. Palve, *Front. Mater.*, **2019**, *6*, 1–7. [crossref], [Google Scholar], [Publisher]
[19] D Denzler, M. Olschewski, K. Sattler, *Applied Physics*, **1998**, *84*, 2841. [crossref], [Google Scholar], [Publisher]
[20] P. Iranmanesh, S. Saeednia, M. Nourzpoor, *Chin. Phys. B*, **2015**, *24*, 046104. [crossref], [Google Scholar], [Publisher]
[21] T. Chandel, J. Singh, P. Rajaram, *AIP Conf. Proc.*, **2015**, *1675*, 020032. [crossref], [Google Scholar], [Publisher]
[22] A. Guinier, *X-Ray Diffraction in Crystals, Imperfect Crystals, and Amorphous Bodies*, W. H. Freeman, San-Francisco, **1963**. [Google Scholar]
[23] R.A. Faris, Z.F. Mahdi, M.D. Abd. Husein, *IOP Conf. Ser.: Mater. Sci. Eng.*, **2020**, *871*, 012019. [crossref], [Google Scholar], [Publisher]
[24] J. Tauc, *Amorphous and Liquid Semiconductors*, Plenum Press, New York, **1974**. [Pdf], [Google Scholar], [Publisher]
[25] J.F. Suyver, S.F. Wuister, J.J. Kelly, A. Meijerink, *Nano Lett.*, **2001**, *1*, 429-433. [crossref], [Google Scholar], [Publisher]
[26] Y.Y. Thangam, R. Anitha, B. Kavitha, *Int. J. Appl. Eng. Res.*, **2012**, *1*, 282-286. [crossref], [Google Scholar], [Publisher]
[27] S.B. Qadri, E.F. Skelton, D. Hsu, A.D. Dinsmore, J. Yang, H.F. Gray, B.R. Ratna, *Physical Review* B., **1999**, *60*, 9191. [crossref], [Google Scholar], [Publisher]
[28] E. Gómez-Barojas, E. Sánchez-Mora, C. Castillo-Abriz, E. Flores-Rodríguez, R. Silva-González, *J. Supercond. Nov. Magn.*, **2013**, *26*, 2337-2340. [crossref], [Google Scholar], [Publisher]

How to cite this article: Alaa Abd AL-Zahra*, Abdul Kareem Mohammed Ali Al-Sammarraie. Hydrothermal synthesis and characterization of zinc sulfide nanoparticles. *Eurasian Chemical Communications*, 2021, 3(9), 606-613.
Link: http://www.echemcom.com/article_134631.html